Available online at www.sciencedirect.com
SCIENCE DIRECT®
European Journal of Medicinal Chemistry 39 (2004) 1001–1011
EUROPEAN JOURNAL OF MEDICINAL CHEMISTRY
www.elsevier.com/locate/ejmech

Original article

4-Anilinoquinazolines with Lavendustin A subunit as inhibitors of epidermal growth factor receptor tyrosine kinase: syntheses, chemical and pharmacological properties

Rica Albuschat [a], Werner Löwe [a,*], Manuela Weber [b], Peter Luger [b], Verena Jendrossek [c]

[a] *Institute of Pharmacy, Free University of Berlin, Königin-Luise-Strasse 2+4, 14195 Berlin, Germany*
[b] *Institute of Crystallography, Free University of Berlin, Takustrasse 6, 14195 Berlin, Germany*
[c] *Department of Radiation Oncology, University of Tübingen, Hoppe-Seyler-Straße 3, 72076 Tübingen, Germany*

Received 11 September 2003; received in revised form 2 March 2004; accepted 11 March 2004

Abstract

4-Anilinoquinazoline derivatives are widely investigated due to their potent epidermal growth factor receptor (EGFR) tyrosine kinase inhibitory activity. Two 4-anilinoquinazolines with Lavendustin A subunit **(10a,b)** were synthesized and examined for their EGFR tyrosine kinase inhibitory activity as well as their antiproliferative properties on variant human cancer cell lines. Both compounds maintained their EGFR tyrosine kinase inhibitory activity at the 10–7 M level and led to significant growth inhibition in certain leukemia, non-small cell lung cancer (NSCLC), ovarian cancer, renal cancer and breast cancer cell lines with GI_{50} values at the 10–6 M level. There could not be observed any notable difference between **10a** and **10b** regarding to their antiproliferative activity. Interestingly, we observed the high tendency of **10a** and **10b** to include certain solvents, e.g. water, DMF, DMSO, which may be due to the remarkable number of hydrogen accepting/donating groups in **10a** and **b**. An X-ray analysis of **10a** including water and DMF illustrates a possible hydrogen bond pattern and could serve as information for preferred receptor (e.g. EGFR tyrosine kinase) binding sites. Finally, we aimed for irreversible EGFR tyrosine kinase inhibitors. The *p*-quinone derivatives **11a** and **11b**, which contain a Michael acceptor position according to the irreversible inhibitor CI-1033, could be derived from the *p*-hydroquinone derivatives **10a** or **10b**, respectively, by oxidation. However, due to their instability **11a** and **11b** could not be obtained in a pure form.

Keywords: 4-Anilinoquinazolines; Salicylanilides; Quinones; Inclusion of solvents; EGFR tyrosine kinase inhibitory activity; Antiproliferative effects

1. Introduction

Growth of malignant tumours is mostly caused by a deregulation of the balance between proliferation, survival and death pathways. In this context, extracellular growth factors (e.g. EGF, TGF-α) bind to their respective cell surface receptors (e.g. EGFR) and activate a network of signaling cascades triggering complex cellular functions such as cell cycle progression, proliferation, survival, invasion, metastasis and angiogenesis [1,2].

It has been shown that up-regulated activity of EGFR correlates with the malignant phenotype of many human epithelial tumours. Therefore, the EGFR signaling represents an attractive target for the design of novel anticancer drugs [3–6]. Therapeutic strategies to inhibit EGFR mediated signaling include antibodies against the ligand binding extracellular receptor domain (cetuximab) as well as small pharmacological inhibitors of the receptor tyrosine kinase Iressa™**1** (Gefitinib, ZD1839) and Tarceva™**2** (Erlotinib, OSI-774), which are acting as reversible antagonists, as well as the irreversible inhibitor CI-1033 (compound **12**, Fig. 1).

Abbreviations: EGFR, epidermal growth factor receptor; PDGFR, platelet derived growth factor receptor; RPTK, receptor protein tyrosine kinase; EGF, epidermal growth factor; TGF-α, transforming growth factor-α; Cys, cysteine; Tyr, tyrosine; ptyr, phosphorylation rate; r.t., room temperature; m.p., melting point; calc., calculated; det., determined; n.t., not tested; NSCLC, Non-small cell lung cancer; IC_{50}, drug concentration resulting in a 50% inhibition of the EGFR tyrosine kinase; GI_{50}, drug concentration resulting in a 50% growth inhibition; TGI, drug concentration resulting in total growth inhibition; LC_{50}, drug concentration resulting in a 50% reduction in the measured protein at the end of drug treatment as compared to that at the beginning; abl kinase, ableson protein tyrosine kinase.

* Corresponding author. Tel.: +49 30 83855280; fax: +49 30 83853854.
E-mail address: wloewe@zedat.fu-berlin.de (W. Löwe).

0223-5234/$ - see front matter © 2004 Elsevier SAS. All rights reserved.
doi:10.1016/j.ejmech.2004.03.010

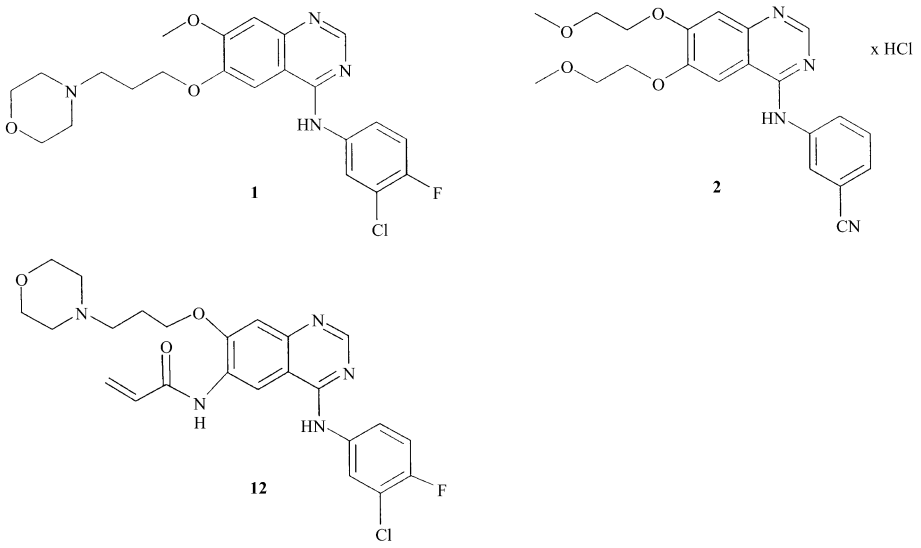

Fig. 1. The 4-anilinoquinazolines Iressa™ **(1)**, Tarceva™ (**2**) and CI-1033 **(12)**.

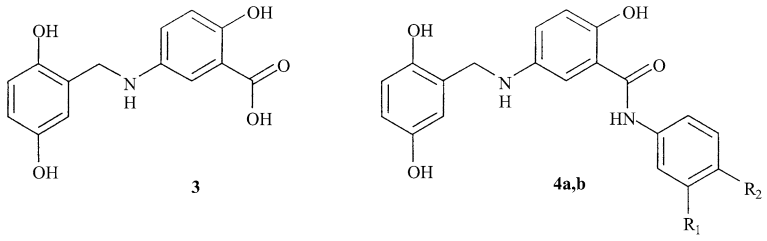

Fig. 2. The Lavendustin A pharmacophore **(3)** and the related salicylanilides **4a** (R_1=Br, R_2=H) and **4b** (R_1=Cl, R_2=F).

Since aberrantly increased EGFR signaling has been shown to interfere with cytotoxic therapies, inhibition of EGFR signaling may not only reduce growth, angiogenesis, invasion and metastasis of tumour cells but also increase sensitivity to cytotoxic therapies [7–9].

Recently, we designed the salicylanilides **4a** and **4b**, which are derivatives of the Lavendustin A pharmacophore **3** (Fig. 2) [10,11]. The anilides **4a** and **4b** (Fig. 2) showed in vitro EGFR tyrosine kinase inhibitory activities of 90% and 96% at a concentration of 10 μM. The *N*-(3-bromophenyl) derivative was tested at 0.1 μM, too. At this concentration it still led to an inhibition of 42% [10].

According to the results of Hodge and Traxler that revealed a bioisosteric relationship between the salicylic group and the quinazoline (illustrated in Fig. 3), we synthesized the 4-anilinoquinazolines with a 6-[(2,5-dihydroxybenzyl)-amino] side chain **10a** and **10b** (Fig. 3) [12,13].

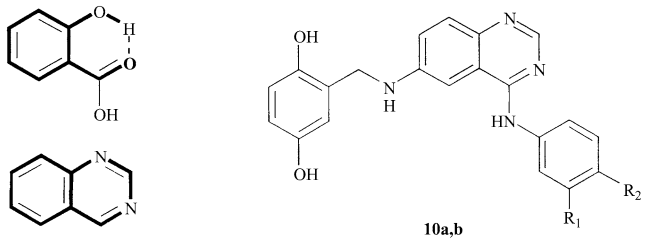

Fig. 3. Salicylic acid and quinazoline as bioisosters and the compounds **10a** (R_1=Br, R_2=H) and **10b** (R_1=Cl, R_2=F).

Based on results of other 4-anilinoquinazoline derivatives, e.g. Iressa™, which emphasized the relevance of the 4-anilinoquinazoline partial structure as an important pharmacophore group of EGFR tyrosine kinase inhibitors [14], we suggested increased EGFR tyrosine kinase inhibitory activities of **10a** and **10b** in comparison to **4a** and **4b**. In addition, the putative improved cellular penetration of **10a** and **10b** in comparison to the salicylanilides **4a** and **4b** together with promising results obtained with Iressa™ we hoped for cytotoxic qualities of **10a** and **10b** [8,15].

A second aim of the present study was to obtain irreversible EGFR tyrosine kinase inhibitor derivatives from **10a** and **10b**, since the diphenolic partial structure in the 6-benzylamino side chain provides the opportunity to get to the corresponding *p*-quinone derivatives **11a** and **11b** by a simple oxidation reaction.

The compounds **11a** and **11b** (Scheme 2) contain a Michael acceptor position on C2 of the quinone that is comparable to that in the 6-acrylamido side chain of the irreversible EGFR tyrosine kinase inhibitor CI-1033 (Fig. 1, Scheme 2). CI-1033 is believed to irreversibly inhibit the EGFR tyrosine kinase by forming a covalent bond to Cys 773 in the ATP binding pocket [16]. CI-1033, which is currently tested in clinical trials for anticancer treatment, has been shown to irreversibly inhibit the EGFR tyrosine kinase with a remarkable IC_{50} value of 1.5 nM [17–20].

Thus, because of the putative irreversible activity of the quinones **11a** and **11b** we hoped for an increased anti-EGFR

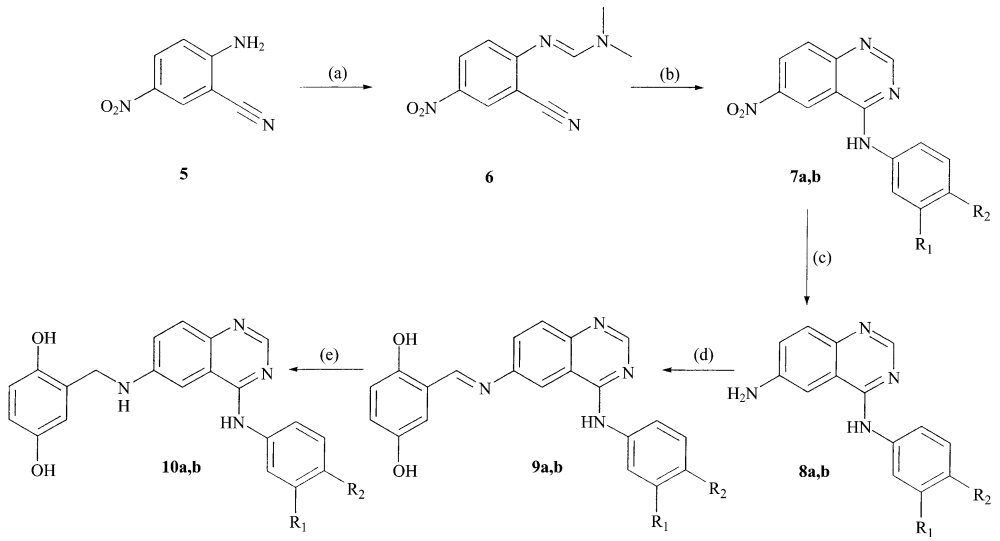

Scheme 1. Synthesis of **10a** (**7–10a**: R_1=Br, R_2=H) and **10b** (**7–10b**: R_1=Cl, R_2=F): (a) dimethylformamide dimethyl acetal, 100 °C, 90 min; (b) 3-bromoaniline or 3-chloro-4-fluoroaniline, acetic acid, reflux, 60 min; (c) iron, acetic acid/ethanol, reflux, 4 h; (d) 2,5-dihydroxybenzaldehyde, acetic acid/ethanol, reflux 2 h; (e) dimethylamine borane, acetic acid, 25 °C.

effectiveness of these two compounds in comparison to the reversible inhibitors **10a** and **10b**.

2. Chemistry

2.1. Syntheses of *10a* and *10b*

Commercial available 5-nitroanthranilo nitrile **(5)** was converted into the corresponding formamidine **6** using dimethylformamide dimethyl acetal. The following reflux boiling of **6** with 3-bromoaniline or 3-chloro-4-fluoroaniline, respectively, in acetic acid gave the 6-nitro-4-phenylaminoquinazoline derivatives **7a,b**. Reduction of the nitro group of **7a,b** with iron in a mixture of acetic acid and ethanol yielded the intermediate 6-aminoquinazolines **8a,b** (step 1–3: [21]).

The Schiff bases **9a,b** were prepared by condensation of **8a,b** with 2,5-dihydroxy-benzaldehyde in a refluxing mixture of acetic acid and ethanol. The following reduction of the imines **9a,b** with dimethylamine borane in glacial acetic acid gave the obtained 6-[(2,5-dihydroxybenzyl)-amino] derivatives **10a** and **10b** (Scheme 1) [22].

2.2. Inclusion of solvents by *10a* and *10b*

Surprisingly, we observed a high tendency of **10a,b** to include certain solvents, such as dimethylformamide (DMF), dimethylsulfoxide (DMSO) and water, and proved that by ^{1}H-NMR-(additional peaks of DMF/DMSO) and mass-(molecular peaks of DMF/DMSO) spectra and additionally by X-ray analysis. Fig. 4 shows the X-ray picture of crystals of **10a** including water and DMF.

Fig. 4 shows the molecular structure of **10a** in the crystal co-crystallizing with water and one DMF molecule. All but one possible N–H and O–H donor groups establish intermolecular hydrogen bonds, as illustrated in Fig. 4 by dashed lines (see also Table 1). Two molecules of **10a**, related by a pure translation in *y*-direction are hydrogen bonded via the O(4)–H group of the hydroquinone group to N(13) of the quinazoline ring. O(4) is also acceptor of a hydrogen bond from the water molecule. The opposite phenolic O–H group is also donor (to the oxygen of a DMF molecule) and accep-

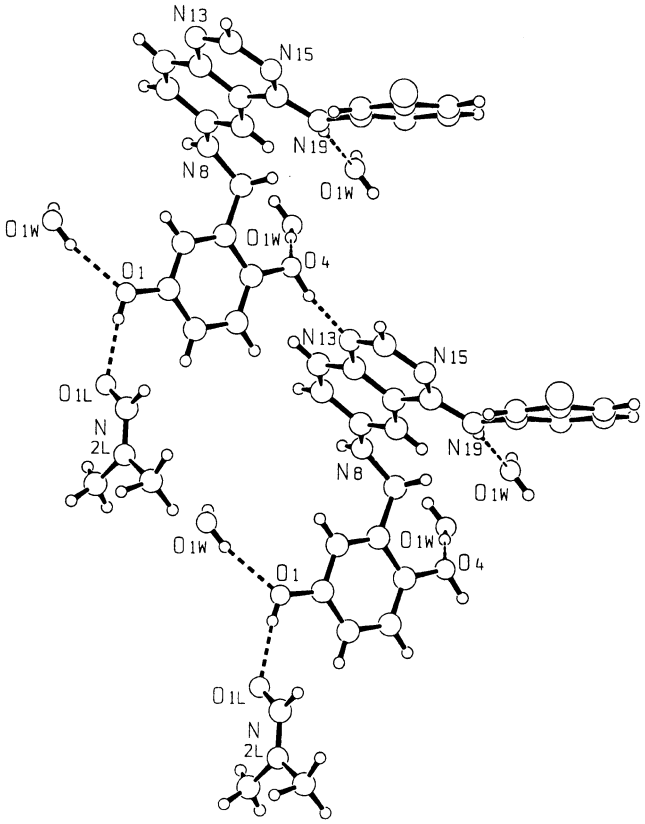

Fig. 4. Crystal structure of **10a** including water and one DMF molecule, hydrogen bonds are indicated by dashed lines, generated with SCHAKAL [23].

Table 1
Hydrogen-bonds in the crystal structure of **10a** including water and one DMF molecule [A and deg.]

D-H...A	D(D–H)	d(H...A)	d(D...A)	<(DHA)	Symmetry
O1-H1...O1L	0.77(3)	1.88(4)	2.641(3)	174.(4)	3–*x*, –*y*, –*z*
O4-H4...N13	0.95(3)	1.69(3)	2.632(3)	169.(3)	*x*,–1 +*y*, *z*
N19-H19...O1W	0.76(3)	2.25(3)	2.994(3)	165.(3)	*x*, *y*, *z*
O1W-H11W...O4	0.85	1.96	2.802(3)	177.	2 – *x*, –*y*, 1 – *z*
O1W-H12W...O1	0.83	2.06	2.886(3)	198.	–1 +*x*, *y*, *z*

tor (from the water molecule) of hydrogen bonds. A further hydrogen bond is formed by the N–H of the 4-[(3-bromophenyl)-amino] substituent to a water molecule. Surprisingly, the possible donor group N(8)-H is not involved in hydrogen bonding in this crystal structure. Although the intermolecular interactions under physiological conditions may be different, the hydrogen bonding pattern found in this structure can serve as information for preferred receptor binding sites.

2.3. Oxidation of the hydroquinone moiety of *10a* and *10b*

In order to obtain irreversible inhibitors we undertook the oxidation of **10a,b**. The resulting quinone partial structure contains a Michael acceptor position (illustrated in Scheme 2).

The electron deficient carbon atom is probably able to form a covalent linkage with the sulfhydryl group of Cys 773 in the ATP binding pocket of the EGFR tyrosine kinase domain, corresponding to the β-carbon in the acrylamido side chain of compound **12** (CI-1033), developed by Pfizer (Scheme 2). CI-1033 was the first irreversible EGFR tyrosine kinase inhibitor reported to be in clinical trials [17–20].

The hydroquinone moiety of **10,b** was easily oxidized by tetra-*n*-butylammonium periodate yielding the quinone derivates **11a,b**. However, due to their instability because of an as yet unknown rearrangement reaction, the desired quinones could not be obtained in a pure form, but mixtures of it with the Schiff bases **9a,b** (Scheme 2).

3. Pharmacology

3.1. EGFR tyrosine kinase inhibitory activity

The determination of the in vitro EGFR tyrosine kinase inhibitory activity was carried out by MDS pharma services, Taiwan (R.O.C.). A431 cell membranes served as the enzyme source and poly (glu/tyr, 4:1) served as the standardized substrate. The phosphorylation rate was determined after incubation of substrate, enzyme and ATP via ELISA in presence (p-tyr_{test}) and in absence (p-tyr_{max}) of inhibitor. The minimal phosphorylation rate (p-tyr_{min}) was determined after incubation of substrate and ATP in absence of enzyme.

The calculation was carried out by the following equation:

$$\text{Inhibition}\left[\,\%\,\right] = 100\ \% - 100\,\% \times \left(\,\text{ptyr}_{\text{test}} - \text{ptyr}_{\text{min}}\,\right)/\left(\,\text{ptyr}_{\text{max}} - \text{ptyr}_{\text{min}}\,\right)$$

3.2. Cytotoxic/cytostatic activity against human malignant glioma cell lines

Growth inhibitory effects of **10a,b** were evaluated in three human malignant glioma cell lines in vitro after 24, 48, 72 and 96 h of continuous drug exposure to the cells using the Wst-1 test [38]. This assay is based on the cleavage of the tetrazolium salt Wst-1 by mitochondrial enzymes that are only active in viable cells. Both drugs were tested at 11 concentrations (100, 75, 50, 25, 12.5, 10, 5, 2.5, 1, 0.5 and 0.1 μM) and dose–response curves were established for each day and each cell line. Growth inhibitory activity of the drugs

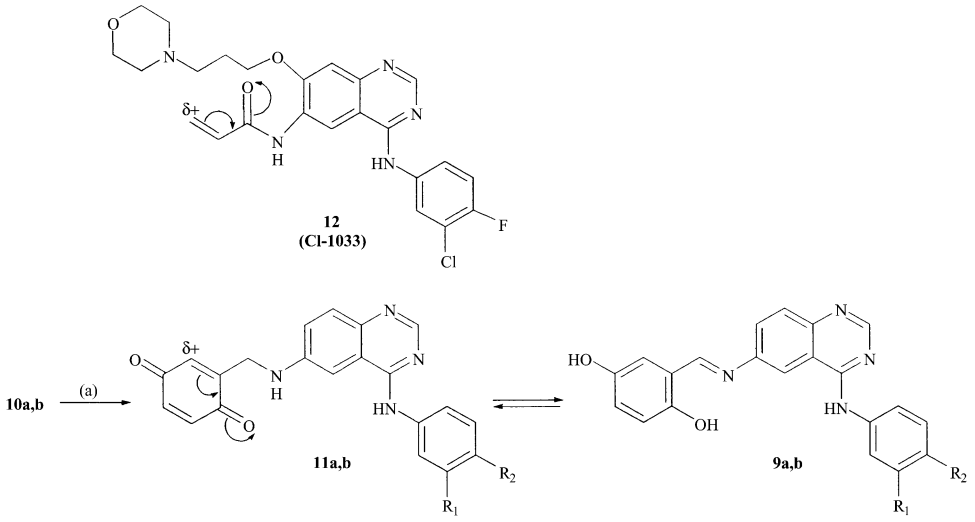

Scheme 2. The irreversible EGFR tyrosine kinase inhibitor CI-1033 (**12**) and the oxidation of the hydroquinone moiety of **10a** and **10b** to obtain the quinone-derivatives **11a** and **11b** as putative irreversible inhibitors (**9–11a**: R_1=Br, R_2=H; **9–11b**: R_1=Cl, R_2=F): (a) tetra-*n*-butyl-ammonium periodate, dichloromethane/methanol, 25 °C, 2 min.

Table 2
EGFR tyrosine kinase inhibitory activities of tested salicylanilides and 4-anilinoquinazolines at a 10, 1 or 0.1 μM concentration, respectively

Compound	R_1	R_2	Inhibitory activity [%]		
			10 μM	1 μM	0.1 μM
4a	Br	H	90	n.t.	42
4b	Cl	F	96	n.t.	n.t.
10a	Br	H	n.t.	65	45
10b	Cl	F	n.t.	71	22
9a			n.t.	58	n.t.

was calculated from dose–response curves (for further details, please refer also to Section 6.3.2.)

3.3. Cytotoxic/cytostatic activity against a panel of 60 human cell lines

The 4-anilinoquinazolines **10a,b** both have been selected by the Evaluation Committee of the National Cancer Institute (NCI), Maryland (USA) for anticancer screening on 60 cell lines.

The determination was carried out following the known in vitro antitumour screening program, which is based upon use of multiple panel of 60 human cell lines [24,25].

The compounds have been tested at five concentrations: 100, 10, 1, 0.1, and 0.01 μM. A 48 h continuous drug exposure protocol is used. The anticancer activity of each compound is deduced from dose–response curves. The response parameters are GI_{50}, TGI and LC_{50}, which are presented in Table 2 according to the data provided by NCI [25].

Further information on the experimental execution is outlined in the experimental Section 6.3.3.

4. Results and discussion

*4.1. EGFR tyrosine kinase inhibitory activity of **4a** and **4b, 9a, 10a** and **10b***

Both 4-anilinoquinazolines **10a** and **10b** (Fig. 5) showed moderate EGFR tyrosine kinase inhibitory activities (Table 2). The imino derivative **9a** (Fig. 5) was at a concentration of 1 μM nearly as active as its amino analogue **10a**.

The hoped-for further increase of the inhibitory activity in comparison to the salicylanilides **4a** and **4b** was not observed. The salicylanilide **4a** is at a concentration of 0.1 μM as active as the corresponding 4-anilinoquinazoline **10a**. This could be valuated as a proof of the supposed bioisosteric relationship of the salicylic group to the quinazoline.

*4.2. Growth inhibitory effects of **10a** and **10b** on U87MG, A172 and T98G cells*

The compounds **10a** and **10b** showed pronounced inhibitory effects on U87MG, A172 and T98G cells. A 50% reduction in the number of viable cells could already be observed upon 24 h of treatment with drug-concentrations ranging from 11 to 30 μM. In this regard, the extent of growth inhibitory action was dependent on the cell line and the drug used.

The highly proliferative U87MG cells were most sensitive to a treatment with the EGFR tyrosine kinase antagonists while A172 cells showed intermediate sensitivity and T98G cells turned out to be most resistant to a treatment with **10a** and **10b** (Fig. 6). In addition, a slight tendency of the cells to be more responsive to a treatment with **10a** than to **10b** could be observed: The drug concentrations required for a reduction of the number of viable cells to 50% of the untreated control cells upon 24, 48, 72 and 96 h of continuous drug treatment (DC_{50}) are given in Table 3.

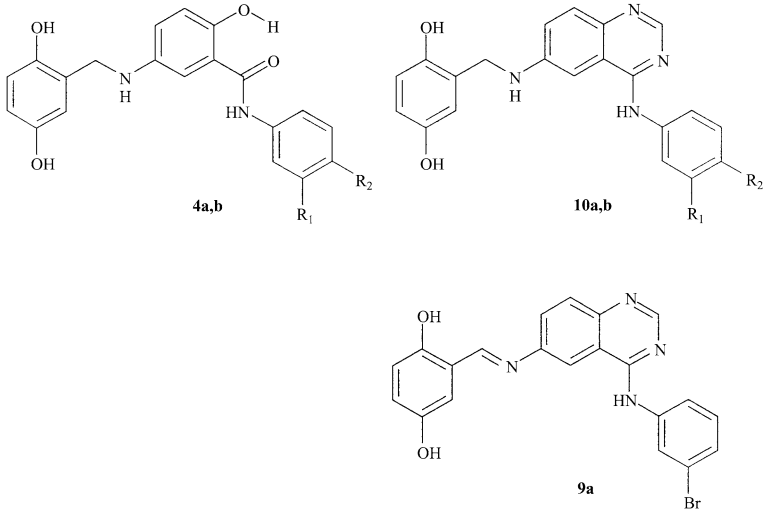

Fig. 5. Tested compounds: **4a** (R_1=Br, R_2=H), **4b** (R_1=Cl, R_2=F), **10a** (R_1=Br, R_2=H), **10b** (R_1=Cl, R_2=F) and **9a**.

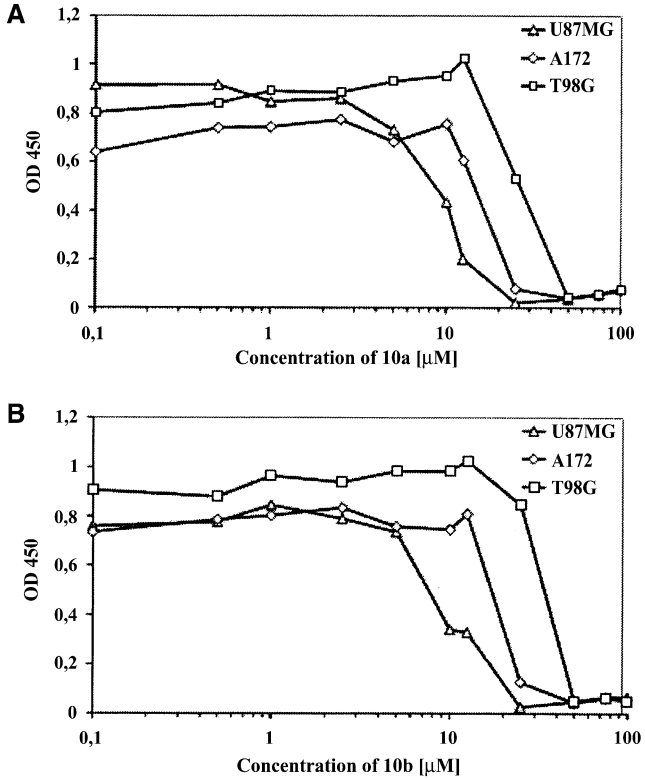

Fig. 6. Human astrocytoma/glioblastoma cell lines differ in their sensitivity to EGF-R antagonists. U87MG, A172 and T98G cells were exposed for 48 h to the indicated concentrations of (a) **10a** or (b) **10b**. Viability was then determined after continuous exposure to the drug by the Wst-1 test. Data represent means of one representative experiment ($n = 3$).

Thus, similar to other cell lines derived from solid human tumors, human astrocytoma/glioblastoma cell lines showed intermediate sensitivity to the antineoplastic effects of 4-anilinoquinazolines with inhibitory activity on EGFR tyrosine kinases. In this context it has to be taken into account that the Wst-1 test evaluates the number of viable cells and does not distinguish between inhibition of proliferation and cytotoxicity. Therefore, the results reflect a combination of cytostatic and direct cytotoxic drug effects.

*4.3. Cytotoxic/cytostatic activity of **10a** and **10b** against a panel of 60 human cell lines*

The results of the evaluation of anticancer activity on **10a,b** are given in Table 4.

Up to 16 cell lines have been shown to be particularly sensitive to a treatment of **10a,b** (GI_{50} at the 0.01 to 1 µM level).

Especially, the growth of the cell lines CCRF-CEM, K-562 and RPMI-8226 (Leukemia), EKVX and NCI-H522 (NSCLC), IGROV1 and SK-OV-3 (Ovarian cancer), A498, ACHN, CAKI-1 (Renal cancer), BT-549 and F47D (Breast cancer) was inhibited at concentrations at the 10–6 M level.

The 3-chloro-4-fluoro derivative **10b** displayed high activity against CCRF-CEM ($GI_{50} = 0.04$ µM, TGI = 0.09 µM), EKVX ($GI_{50} = 0.75$ µM), A498 ($GI_{50} = 0.23$ µM) and ACHN ($GI_{50} = 0.68$ µM) cells.

Additionally, cytotoxic effects—as indicated by the LC_{50} values—can be observed on some cell lines, e.g. *Leukemia* (**10b**: 33.7–98.7 µM), some *NSCLC* (**10a,b**: 51.5–98.7), some *Melanoma* (**10a,b**: 61.4–74.1) and some *Renal* (A498: **10a,b**: 42.4 and 40.8) cells.

The mechanism of the cytotoxic activity is not completely clear. Cancer cells of NSCLC (40–80%), renal tumours (50–90%), glioblastoma (40–50%), ovarian (35–70%) and some breast (14–91%) tumours are known for their EGFR (over)-expression [26].

It is possible, that both compounds are not only cytotoxic/cytostatic because of their EGFR tyrosine kinase inhibitory activity, but act by other mechanisms, e.g. inhibition of other receptor protein tyrosine kinases like the PDGFR tyrosine kinase or of cellular protein kinases like the abl kinase. The abl kinase or its related oncogenic product, the bcr-abl kinase (caused by a chromosome rearrangement resulting in the so-called Philadelphia chromosome) plays an important role in the genesis and progression of leukemias, e.g. 95% of chronic myeloid leukemias are Philadelphia chromosome positive [27]. The 2-phenylaminopyrimidine derivative Glivec used for the treatment of the chronic myeloid leukemia has been shown to act as an ATP antagonist at the abl kinase as well as at the PDGFR tyrosine kinase [28–30]. Since compound **10b** was designed as an ATP antagonist as well, we suggest, that the excellent activities of **10b** on leukemia cell lines could at least be partially due to an inhibition of the abl kinase and/or of the PDGFR tyrosine kinase as well.

5. Conclusions

The 4-anilinoquinazolines **10a** and **10b** are relative potent EGFR tyrosine kinase inhibitors with approximate IC_{50} values in the range of 0.1–1 µM. Additionally, both substances cause antiproliferative to cytotoxic effects on certain human

Table 3
Human astrocytoma/glioblastoma cell lines show a tendency to increased sensitivity to the treatment with **10a**. U87MG, A172 and T98G cells were continuously exposed for 24–96 h to the indicated concentrations of **10a** or **10b**. Viability was then determined by the Wst-1 test. DC_{50} values represent the drug concentration that was required to reduce cell viability as determined by WST-1 reduction to 50% of untreated controls

DC_{50} values [µM]	T98G		A172		U87MG	
	10a	**10b**	**10a**	**10b**	**10a**	**10b**
24 h	33.0	36.5	19.0	21.5	10.1	13.6
48 h	24.5	29.5	15.5	21.8	9.4	10.4
72 h	25.3	33.8	16.0	19.0	8.8	8.3
96 h	28.0	32.3	15.1	19.0	9.4	8.4

Table 4
In vitro testing results of **10a,b**: $GI_{50,}$ TGI and LC_{50} [μM]

Panel/cell line	**10a**			**10b**		
	GI_{50}	TGI [μM]	LC_{50}	GI_{50}	TGI [μM]	LC_{50}
Leukemia						
CCRF-CEM	5.26	8.32	≥100	0.04	0.09	33.7
K-526	2.54	20.5	≥100	2.49	13.8	80.7
RPMI-8226	4.61	20.7	≥100	2.37	6.51	98.7
NSCLC						
A549/ATCC	12.8	36.9	≥100	13.0	37.6	≥100
EKVX	2.19	13.0	54.3	0.75	17.2	51.5
HOP-62	17.1	34.5	69.4	19.3	43.7	98.7
NCI-H226	15.0	29.1	56.6	12.3	25.7	53.8
NCI-H23	22.2	59.5	≥100	54.5	≥100	≥100
NCI-H460	26.0	≥100	≥100	46.2	≥100	≥100
NCI-H522	4.14	≥100	≥100	2.76	≥100	≥100
Colon cancer						
COLO 205	8.67	35.8	≥100	14.1	≥100	≥100
HCC-2998	27.2	≥100	≥100	28.6	≥100	≥100
HCT-116	21.9	≥100	≥100	23.3	≥100	≥100
HCT-15	66.8	≥100	≥100	24.0	≥100	≥100
HT29	35.6	≥100	≥100	29.2	≥100	≥100
SW-620	21.8	89.6	≥100	13.3	≥100	≥100
CNS cancer						
SF-268	13.8	48.8	≥100	23.2	≥100	≥100
SF-295	17.0	37.6	83.1	24.1	53.6	≥100
SF-539	11.2	31.3	88.0	10.7	30.6	87.6
SNB-19	13.0	29.7	67.9	25.3	≥100	≥100
SNB-75	29.7	≥100	≥100	21.9	85.3	≥100
U251	16.1	52.7	≥100	11.4	43.5	≥100
Melanoma						
LOX IMVI	19.2	53.1	≥100	22.3	91.0	≥100
M14	18.4	40.4	88.9	25.6	≥100	≥100
SK-MEL-2	29.9	≥100	≥100	42.1	≥100	≥100
SK-MEL-28	21.0	50.1	≥100	21.5	64.4	≥100
SK-MEL-5	14.7	31.8	68.4	9.22	27.0	74.1
UACC-257	14.3	30.0	62.9	14.7	32.7	72.5
UACC-62	16.9	35.2	73.4	15.4	30.7	61.4
Ovarian cancer						
IGROV1	4.84	≥100	≥100	4.63	≥100	≥100
OVCAR-3	6.75	28.3	95.2	13.3	75.0	≥100
OVCAR-4	31.0	≥100	≥100	25.8	≥100	≥100
OVCAR-5	23.4	82.1	≥100	36.2	≥100	≥100
OVCAR-8	8.01	32.5	≥100	11.9	43.4	≥100
SK-OV-3	4.56	24.1	≥100	6.70	33.4	≥100
Renal cancer						
786-0	14.8	41.6	≥100	13.7	40.4	≥100
A498	1.90	11.8	42.4	0.23	7.57	40.8
ACHN	1.10	26.5	≥100	0.68	22.3	69.6
CAKI-1	1.75	31.4	≥100	2.90	30.4	≥100
RXF 393	15.1	41.1	≥100	16.4	71.9	≥100
SN12C	19.2	66.0	≥100	11.1	34.2	≥100
UO-31	11.1	59.4	≥100	8.76	≥100	≥100
Prostate cancer						
PC-3	10.9	33.0	99.8	13.7	40.8	≥100
DU-145	10.5	34.1	≥100	10.1	26.3	68.4
Breast cancer						
MCF7	29.6	≥100	≥100	55.9	≥100	≥100
NCI/ADR-RES	25.7	≥100	≥100	40.3	≥100	≥100
MDA-MB-231/ATCC	19.6	42.2	90.6	10.4	31.5	95.5
HS 578T	22.4	65.6	≥100	18.4	61.6	≥100
MDA-MB-435	13.9	31.2	69.7	19.6	44.2	99.5
BT-549	4.64	28.0	≥100	9.21	25.5	67.0
T-47D	5.28	41.2	≥100	3.42	45.2	≥100

cancer cell lines. Worthy of remark is, that **10b** showed excellent cytotoxic activity on the leukemia cell line CCRF-CEM with GI_{50} and TGI values at the 0.01 μM levels (0.04 and 0.09 μM) and a LC_{50} value of 33.7 μM.

6. Experimental

6.1. Chemistry

All reagents were fresh, commercial grade chemicals. Melting points (m.p.) were determinated on a Lindström-apparatus and are uncorrected. ^{1}H-NMR spectra were recorded on Bruker AC-300 spectrometer in DMSO-d_6 solutions using tetramethylsilane as an internal reference. Coupling patterns are described as follows: s, singlet; d, doublet, dd, doubled doublet; t, triplet; m, multiplet; and 1H, 2H, 3H, etc. as the number of hydrogen integrated within a given coupling pattern. The chemical shifts *(δ)* were measured to two decimal points and are given in ppm.

^nJ describes a coupling constant with n = numbers of bonds between the coupling hydrogens. If the coupling partner is not a hydrogen, but fluor, this is indicated in parenthesis behind ^nJ. The coupling constants were rounded off to one decimal place.

Elementary analyses were performed on Perkin-Elmer Elementar-Vario EL. The analytical results for the elements C, H, N were within ±0.4% of the theoretical values.

6.1.1. *N′-(2-cyano-4-nitro-phenyl)*-N,N-*dimethylimidoformamide* ***(6)***

According to a published procedure [21] **6** was prepared by reflux boiling of 5-nitroanthranilonitrile **5** (5.00 g, 30.7 mmol) in 20 ml dimethylformamide dimethyl acetal. After 90 min the mixture was allowed to cool to room temperature. The solid was filtered off, washed with several portions of diethyl ether and dried to yield **6** as yellow crystals (6.50 g, 96.9%), m.p. 151 °C (lit. 153–155 °C).

6.1.2. *6-Nitro-4-(3-bromo-phenylamino)-quinazoline* ***(7a)***

The preparation of **7a** was executed according to a published procedure [21]. Therefore, a mixture of **6** (5.00 g, 22.9 mmol) and 3-bromoaniline (3.94 g, 22.9 mmol) was refluxed in glacial acetic acid. After 60 min the mixture was filtered hot. The solid was washed with diethyl ether and dried to yield **7a** as yellow crystals (6.05 g, 76.5%), m.p. ≥ 250 °C (dec., lit. 267–270 °C).

6.1.3. *6-Nitro-4-(3-chloro-4-fluoro-phenylamino)-quinazoline* ***(7b)***

Compound **7b** was obtained similarly to **7a** from compound **6** (5.00 g, 22.9 mmol) and 3-chloro-4-fluoroaniline (3.33 g, 22.9 mmol) as yellow crystals (5.65 g, 77.3%), m.p. ≥ 239 °C (dec.). ^{1}H-NMR (400 MHz): 10.49 (s, 1H, anilino-N*H*, exchanged by D_2O), 9.60 (d, ^4J = 1.7 Hz, 1H, quinazolineH_5), 8.75 (s, 1H, quinazolineH_2), 8.55 (dd, ^3J = 9.2 Hz, ^4J = 2.2, 1H, quinazolineH_7), 8.17 (d, ^4J (H, F) = 4.6 Hz, 1H, anilinoH_2), 7.98 (d, ^3J = 9.2 Hz, 1H, quinazolineH_8), 7.90.7.73 (m, 1H, anilinoH_6), 7.61.7.34 (m, 1H, anilinoH_5). Anal. $C_{14}H_8ClFN_4O_2$.

6.1.4. N^4*-(3-Bromo-phenyl)-4,6-quinazolinediamine* ***(8a)***

Following a published procedure [21] **8a** was prepared by reduction of **7a** with iron: To a heavy stirred mixture of **7a** (11.00 g, 31.9 mmol) in ethanol (55 ml) and acetic acid (15 ml) was added iron (8.80 g, 157.6 mmol). The resulting mixture was heated to reflux for 3 h. After cooling to room temperature 80 ml water was added to the mixture. The solid was filtered off and washed several times with water. Then 200 ml ethyl acetate was added to the residue. The resulting mixture was first washed with 25% $KHCO_3$ solution, then twice with brine, dried over anhydrous Na_2SO_4, decolourized with charcoal and filtered. The filtrate was concentrated in vacuum. The crude product was purified by flash chromatography over silica gel (ethyl acetate) to yield **8a** as yellow crystals (5.52 g, 54.8%), m.p. 203–204 °C (lit. 203.5–204.5 °C).

6.1.5. *N^4-(3-Chloro-4-fluoro-phenyl)-4,6-quinazolinediamine* ***(8b)***

Compound **7b** (10.00 g, 31.4 mmol) was reduced similarly to **7a** by iron (8.80 g, 157.6 mmol) to give **8b** as yellow crystals (2.80 g, 30.9%), m.p. 244 °C. ^{1}H-NMR (400 MHz): 9.47 (s, 1H, anilino-N*H*, exchanged by D_2O), 8.35 (s, 1H, quinazolineH_2), 8.20 (dd, ^4J = 2.6 Hz, ^4J (H, F) = 6.9 Hz, 1H, anilinoH_2), 7.83 (m, 1H, anilinoH_6), 7.54 (d, ^3J = 8.9 Hz, 1H, quinazolineH_8), 7.41 (t, ^3J (H, F) = 9.1 Hz, 1H, anilinoH_5), 7.31 (d, ^4J = 2.3 Hz, 1H, quinazolineH_5), 7.24 (dd, ^3J = 8.8 Hz, ^4J = 2.2 Hz, 1H, quinazolineH_7), 5.62 (s, 1H, quinazolineNH_2, exchanged by D_2O). Anal. $C_{14}H_{10}ClFN_4$.

6.1.6. *2-{[4-(3-Bromo-phenylamino)-quinazolin-6-ylimino]-methyl}-benzene-1,4-diol* ***(9a)***

A mixture of **8a** (2.00 g, 6.4 mmol) and 2,5-dihydroxybenzaldehyde (0.88 g, 6.4 mmol) was refluxed in 45 ml of a mixture of ethanol and glacial acetic acid (1:1) for 2.5 h. The ethanol was then removed in vacuum. The residual mixture was poured onto ice, neutralized with Na_2CO_3 solution and extracted with ethyl acetate. The combined extracts were washed with water, dried over anhydrous Na_2SO_4 and the solvent was removed in vacuum. The crude product was purified by recrystallization from dichloromethane/methanol (9 + 1) to yield **9a** as yellow-orange powder (2.11 g, 76.5%), m.p. 243–246 °C (dec.). ^{1}H-NMR (400 MHz): 12.09 (s, 1H, 1,4-Di-OH-ArOH_1, exchanged by D_2O), 9.90 (s, 1H, anilino-N*H*, exchanged by D_2O), 9.17 (s, 1H, 1,4-Di-OH-ArOH_4, exchanged by D_2O), 9.03 (s, 1H, 1,4-Di-OH-ArC*H*), 8.65 (s, 1H, quinazolineH_2), 8.52 (d, ^4J = 2.0 Hz, 1H, quinazolineH_5), 8.26 (s, 1H, anilinoH_2), 8.02 (dd, ^3J = 8.8 Hz, ^4J = 2.0 Hz, 1H, quinazolineH_7), 7.95 (d, ^3J = 8.2 Hz, 1H, anilinoH_4), 7.88 (d, ^3J = 8.9 Hz, 1H, quinazolineH_8), 7.39 (t, ^3J = 8.0 Hz, 1H, anilinoH_5), 7.30 (d, ^3J = 8.2 Hz, 1H,

anilinoH_6), 7.11 (d, ^4J = 2.9 Hz, 1H, 1,4-Di-OH-ArH_5), 6.92 (dd, ^3J = 8.9 Hz, ^4J = 2.9 Hz, 1H, 1,4-Di-OH-ArH_3), 6.84 (d, ^3J = 8.9 Hz, 1H, 1,4-Di-OH-ArH_2). Anal. $C_{21}H_{15}BrN_4O_2$.

*6.1.7. 2-{[4-(3-Chloro-4-fluoro-phenylamino)-quinazolin-6-ylimino]-methyl}-benzene-1,4-diol **(9b)***

Compound **9b** was obtained similarly to **9a** from **8b** (1.00 g, 3.5 mmol) and 2,5-dihydroxybenzaldehyde (0.48 g, 3.5 mmol). The crude product was purified by recrystallization from dichloromethane/methanol (9 + 1) to yield **9b** as an orange powder (1.10 g, 77.5%), m.p. 257 °C. ^{1}H-NMR (400 MHz): 12.09 (s, 1H, 1,4-Di-OH-ArOH_1, exchanged by D_2O), 9.94 (s, 1H, anilino-N*H*, exchanged by D_2O), 9.17 (s, 1H, 1,4-Di-OH-ArOH_4, exchanged by D_2O), 9.03 (s, 1H, 1,4-Di-OH-ArC*H*), 8.65 (s, 1H, quinazolineH_2), 8.49 (d, ^4J = 2.2 Hz, 1H, quinazolineH_5), 8.24 (dd, ^4J = 2.6 Hz, ^4J (H, F) = 6.9 Hz, 1H, anilinoH_2), 8.00 (dd, ^3J = 9.2 Hz, ^4J = 2.1 Hz, 1H, quinazolineH_7), 7.93.7.79 (m, 2H, quinazolineH_8, anilinoH_6), 7.48 (t, ^3J (H, F) = 9.1 Hz, 1H, anilinoH_5), 7.11 (d, ^4J = 2.9 Hz, 1H, 1,4-Di-OH-ArH_5), 6.92 (dd, ^3J = 8.7 Hz, ^4J = 2.9 Hz, 1H, 1,4-Di-OH-ArH_3), 6.84 (d, ^3J = 8.9 Hz, 1H, 1,4-Di-OH-ArH_2). Anal. $C_{21}H_{14}ClFN_4O_2 \cdot 0.5H_2O$.

When the crude product was dissolved in dimethylformamide and then purified by flash chromatography on silica gel (ethyl acetate/*n*-hexane, 9:1), **9b(DMF)** was obtained, which contained 1 mol water and 1 mol dimethylformamide per mol **9b**. 12.08 (s, 1H, 1,4-Di-OH-ArOH_1, exchanged by D_2O), 9.94 (s, 1H, anilino-N*H*, exchanged by D_2O), 9.17 (s, 1H, 1,4-Di-OH-ArOH_4, exchanged by D_2O), 9.03 (s, 1H, 1,4-Di-OH-ArC*H*), 8.65 (s, 1H, quinazolineH_2), 8.49 (d, ^4J = 1.7 Hz, 1H, quinazolineH_5), 8.22 (dd, ^4J = 2.5 Hz, ^4J (H, F) = 6.8 Hz, 1H, anilinoH_2), 8.01 (dd, ^3J = 8.9 Hz, ^4J = 1.9 Hz, 1H, quinazolineH_7), 7.95 (s, 1H, DMF-C*H*) 7.92.7.82 (m, 2H, quinazolineH_8, anilinoH_6), 7.48 (t, ^3J (H, F) = 9.1 Hz, 1H, anilinoH_5), 7.12 (d, ^4J = 2.8 Hz, 1H, 1,4-Di-OH-ArH_5), 6.91 (dd, ^3J = 8.8 Hz, ^4J = 2.8 Hz, 1H, 1,4-Di-OH-ArH_3), 6.85 (d, ^3J = 8.8 Hz, 1H, 1,4-Di-OH-ArH_2), 2.89 (s, 3H, DMF-CH_3), 2.73 (s, 3H, DMF-CH_3).

*6.1.8. 2-{[4-(3-bromo-phenylamino)-quinazolin-6-ylamino]-methyl}-benzene-1,4-diol **(10a)***

Dimethylamine borane (0.14 g, 2.4 mmol) was dissolved in 10 ml glacial acetic acid and added dropwise to a cooled (0–5 °C) suspension of **9a** (1.0 g, 2.3 mmol) in glacial acetic acid. The mixture was stirred at room temperature for 60 min, then poured onto ice and neutralized with 5N NaOH. The solid was collected, washed with water and dried. The resulting crude product was recrystallized from dichloromethane/methanol (9+1) to yield **10a** as yellow powder (0.77 g, 76.5%), m.p. 231 °C (dec). ^{1}H-NMR (400 MHz): 9.41 (s, 1H, anilinoN*H*, exchanged by D_2O), 8.88 (s, 1H, 1,4-Di-OH-ArOH_1, exchanged by D_2O), 8.61 (s, 1H, 1,4-Di-OH-ArOH_4, exchanged by D_2O), 8.38 (s, 1H, quinazolineH_2), 8.16 (d, ^4J = 1.8 Hz, 1H, anilinoH_2), 7.88 (d, ^3J = 8.2 Hz, 1H, anilinoH_4), 7.54 (d, ^3J = 9.0 Hz, 1H, quinazolineH_8), 7.37 (dd, ^3J = 9.1 Hz, ^4J = 2.1 Hz 1H, quinazolineH_7), 7.34.7.31 (t, ^3J = 8.1 Hz, 1H, anilinoH_5), 7.29 (d, ^4J = 1.9 Hz, 1H, quinazolineH_5), 7.24 (d, ^3J = 8.1 Hz, 1H, anilinoH_6), 6.71 (d, ^4J =2.8 Hz, 1H, 1,4-Di-OH-ArH_5), 6.65 (d, ^3J = 8.6 Hz, 1H, 1,4-Di-OH-ArH_2), 6.48 (dd, ^3J = 8.5 Hz, ^4J = 2.9 Hz, 1H, 1,4-Di-OH-ArH_4), 6.41 (t, ^3J = 5.6 Hz, 1H, quinazoline-N*H*, exchanged by D_2O), 4.31 (d, ^3J = 5.5 Hz, 2H, 1,4-Di-OH-ArCH_2). Anal. $C_{21}H_{17}BrN_4O_2 \cdot H_2O$.

*6.1.9. 2-{[4-(3-chloro-4-fluoro-phenylamino)-quinazolin-6-ylamino]-methyl}-benzene-1,4-diol **(10b)***

Compound **9b(DMF)** (1.50 g, 3.0 mmol) was reduced similarly to **9a** by dimethylamine borane (0.20 g, 3.4 mmol) to yield **10b(DMF)**, which contained 1 mol water and 1 mol dimethylformamide per mol **10b**. Compound **10b(DMF)** was obtained as bride yellow crystals (1.10 g, 70.5%), m.p. 230 °C (dec.). ^{1}H-NMR (400 MHz): 9.44 (s, 1H, anilino-N*H*, exchanged by D_2O), 8.88 (s, 1H, 1,4-Di-OH-ArOH_1, exchanged by D_2O), 8.62 (s, 1H, 1,4-Di-OH-ArOH_4, exchanged by D_2O), 8.36 (s, 1H, quinazolineH_2), 8.13 (dd, ^4J (H, F) = 6.9 Hz, ^4J = 2.6 Hz, 1H, anilinoH_2), 7.95 (s, 1H, DMF-C*H*), 7.85.7.76 (m, 1H, anilinoH_6), 7.55 (d, ^3J = 9.0 Hz, 1H, quinazolineH_8), 7.46.7.34 (m, 2H, anilinoH_5, quinazolineH_7), 7.27 (d, ^4J = 2.2 Hz, 1H, quinazolineH_5), 6.71 (d, ^4J =2.9 Hz, 1H, 1,4-Di-OH-ArH_5), 6.65 (d, ^3J = 8.5 Hz, 1H, 1,4-Di-OH-ArH_2), 6.49 (dd, ^3J = 8.5 Hz, ^4J = 2.9 Hz, 1H, 1,4-Di-OH-ArH_3), 6.41 (t, ^3J = 5.6 Hz, 1H, quinazoline-N*H*, exchanged by D_2O), 4.31 (d, ^3J = 5.6 Hz, 2H, 1,4-Di-OH-CH_2), 2.89 (s, 3H, DMF-CH_3), 2.73 (s, 3H, DMF-CH_3). Anal. $C_{21}H_{16}ClFN_4O_2 \cdot C_3H_7NO \cdot H_2O$.

Removal of the included solvents is possible by recrystallization from ethanol/petrolether. Pale yellow powder, m.p. 214 °C. ^{1}H-NMR (400 MHz): 9.44 (s, 1H, anilino-N*H*, exchanged by D_2O), 8.88 (s, 1H, 1,4-Di-OH-ArOH_1, exchanged by D_2O), 8.62 (s, 1H, 1,4-Di-OH-ArOH_4, exchanged by D_2O), 8.36 (s, 1H, quinazolineH_2), 8.13 (dd, ^4J (H, F) = 6.9 Hz, ^4J = 2.6 Hz, 1H, anilinoH_2), 7.86.7.75 (m, 1H, anilinoH_6), 7.55 (d, ^3J = 9.0 Hz, 1H, quinazolineH_8), 7.43 (t, ^3J (H, F) = 9.2 Hz, 1H, anilinoH_5), 7.36 (dd, ^3J = 9.0 Hz, ^4J = 2.2 Hz, 1H, quinazolineH_7), 7.27 (d, ^4J = 2.2 Hz, 1H, quinazolineH_5), 6.71 (d, ^4J =2.9 Hz, 1H, 1,4-Di-OH-ArH_5), 6.65 (d, ^3J = 8.5 Hz, 1H, 1,4-Di-OH-ArH_2), 6.49 (dd, ^3J = 8.5 Hz, ^4J = 2.9 Hz, 1H, 1,4-Di-OH-ArH_3), 6.41 (t, ^3J = 5.6 Hz, 1H, quinazoline-N*H*, exchanged by D_2O), 4.31 (d, ^3J = 5.6 Hz, 2H, 1,4-Di-OH-ArCH_2). Anal. $C_{21}H_{16}ClFN_4O_2$.

6.2. X-ray crystal structure analysis

After several attempts with different solvent combinations small crystals of **10a** were successfully obtained by vapour diffusion from DMF/acetone. Diffraction data of a crystal with dimension 0.24 × 0.20 × 0.10 mm were collected at 100 K on a Bruker SMART 1000 difractometer with MoKα-radiation (graphite monochromator, λ = 0.7107 Å) and CCD

area detector. The crystal lattice is triclinic, space group P1bar, and unit cell parameters $a = 8.572(1)$, $b = 11.249(1)$, $c = 12.800(1)$ Å, $\alpha = 82.78(2)$, $\beta = 84.10(2)$, $\gamma = 76.19(2)°$, $V = 1185.7(14)$ Å^3, $Z = 2$, $d_{calc} = 1.480$ g × cm^{-3}, $\mu = 1.775$ mm^{-1}.

The 14636 reflections were collected up to $2\theta_{max} = 62°$ and reduced to 7155 independent reflections ($R_{int} = 0.034$). The phase problem was solved with direct methods (SIR92) [31], the structure was refined on F^2 with SHELXL with anisotropic displacement parameters for the non H atoms [32]. The hydrogens which were located from difference syntheses were given isotropic displacement parameters. The asymmetric unit was found to consist of one molecule **10a**, one DMF molecule and one water molecule. An absorption correction was also applied (SADDABS) [33]. After convergence of the refinements discrepancy factors were $R_1 = 0.0444$, $wR_2 = 0.0983$ for $I > 2\sigma(I)$ and $R_1 = 0.0823$, $wR_2 = 0.1076$ for all data, Gof = 0.987.

6.3. Pharmacology

6.3.1. In vitro EGFR tyrosine kinase activity

The EGFR tyrosine kinase inhibitory activity assay was carried out by MDS Pharma Services, Taiwan (R.O.C.).
Enzyme source: Human A431 cells
Substrate: 10 μg/ml Polyglutamic acid/tyrosine [poly(glu/ptyr, 4:1)]
Vehicle: 1% dimethylsulfoxide
Pre-incubation time/temp.: None
Incubation time/temp.: 60 min/25 °C
Incubation buffer: 50 mM Hepes, 20 mM $MgCl_2$, 0.2 mM Na_3VO_4, pH 7.4
Quantitation Method: ELISA quantitation of Poly (glu: ptyr)
Significance Criteria: ≥50% of maximal stimulation or inhibition

The epidermal growth factor receptor was purchased from Sigma (prod. number: E2645). The enzyme assay was performed in wells coated with poly(glu/tyr) substrate. Incubation buffer and test compound were added into the wells. Finally, enzyme was added and then ATP to start the reaction.

For the calculation of the inhibitory activities, each assay contained two wells for determination of the maximum phosphorylation rate ($ptyr_{max}$: in the absence of inhibitor) and two wells for determination of the minimum phosphorylation rate ($ptyr_{min}$: in the absence of enzyme), as well. Quantitation of phospho-tyrosine was determined via ELISA [34–37].

6.3.2. Determination of cytostatic/cytotoxic activity in human malignant glioma cell lines

Cell lines: The human astrocytoma/glioblastoma cell lines A172, U87MG and T98G were obtained from ATCC (Rockville, MD, USA). All cell lines were adapted to RPMI1640 medium containing 2 mM glutamine and 2 g/l sodium bicarbonate (PAA, Linz, Austria) supplemented with 10% (v/v) heat-inactivated fetal bovine serum and 100 U/ml penicillin and 100 μg/ml streptomycin (Life Technologies, Karlsruhe, Germany). All cell lines were grown as monolayers in tissue culture flasks in a humidified atmosphere (5% CO_2/95% air) at 37 °C.

Determination of cell viability: Drug sensitivity assessment was performed with cells by the Wst-1 cell proliferation reagent (Roche Molecular Biochemicals, Mannheim, Germany) as described elsewhere [38]. In brief, cells were seeded in 96-well plates. Twenty-four hours after plating, the drugs were diluted in culture medium and added to the cells. For evaluation of the antiproliferative and cytotoxic effects, human astrocytoma/glioblastoma cell lines (U87MG, A172 and T98G) were exposed for 24–96 h to 0.1–100 μM **10a** or **10b**. Viability was determined after continuous exposure to the drug of interest for the indicated times by addition of Wst-1 solution. Absorbance at 450 nm (λ reference: 620 nm) was determined upon incubation of the cells at 37 °C in the presence of the Wst-1 solution for 60 min using a Anthos 2010 plate reader (Anthos, Krefeld, Germany). The DC50 represents the drug concentration causing a reduction in the number of viable cells to 50% of untreated control cells.

6.3.3. Evaluation for cytotoxic activity against a panel of 60 human cancer cell lines

Evaluation of anticancer activity was performed at the National Cancer Institute (Bethesda, MD, USA).

The compounds were tested in an in-vitro 60-cell line anticancer assay over a 5 log dose range. The cell lines are derived from nine human cancer types: leukemia, NSCLC, colon, CNS, melanoma, ovarian, renal, prostate and breast.

The tumour cell lines are grown in RPMI 1640 medium containing 5% fetal bovine serum and 2 ml L-glutamine. For a typical screening experiment, cells are inoculated into 96 well microtiter plates in 100 μM at plating densities ranging from 5000 to 40 000 cells/well depending on the doubling time of individual cell lines. After cell inoculation, the microtiter plates are incubated at 37 °C, 5% CO_2, 95% air and 100% relative humidity for 24 h prior to addition of experimental drugs.

After 24 h, two plates of each cell line are fixed in situ with TCA, to represent a measurement of the cell population for each cell line at the time of drug addition (Tz).

Experimental drugs are solubilized in DMSO at 400-fold the desired final maximum test concentration. At the time of drug addition, an aliquot of concentrate is thawed and diluted to twice the desired final maximum test concentration with complete medium containing 50 μg/ml gentamicin. Additional four, 10-fold or 1/2 log serial dilutions are made to provide a total of five drug concentrations plus control. Aliquots of 100 μl of these different drug dilutions are added to the appropriate microtiter wells already containing 100 μl of medium, resulting in the required final drug concentration.

Following drug addition, the plates are incubated for an additional 48 h at the above-mentioned conditions. For adherant cells, the assay is terminated by the addition of cold TCA.

Cells are fixed in situ by the gentle addition of 50 µl of cold 50% (w/v) TCA (final concentration, 10% TCA) and incubated for 60 min at 4 °C. The supernatant is discarded, and the plates are washed five times with tap water and air dried. Sulforhodamine B (SRB) solution (100 µl) at 0.4% (w/v) in 1% acetic acid is added to each well, and plates are incubated for 10 min at room temperature. After staining, unbound dye is removed by washing five times with 1% acetic acid and the plates are air dried. Bound stain is subsequently solubilized with 10 mM trizma base, and the absorbance is read on an automatic plate reader at a wavelength of 515 nm.

For suspension cells, the methodology is the same except that the assay is terminated by fixing settled cells at the bottom of the wells by gently adding 50 µl of 80% TCA (final concentration, 16% TCA).

Using the seven absorbance measurements [time zero, (T_z), control growth, *(C)*, and test growth in the presence of drug at the five concentration levels, (T_i)], the percentage growth is calculated at each of the drug concentrations levels.

Percentage growth is calculated as: $[(T_i - T_z)/(C - T_z)]\times 100$ for concentrations for which $Ti \geq Tz$ and $[(T_i - T_z)/T_z]\times 100$ for concentrations for which $T_i < T_z$.

Three dose response parameters are calculated for each experimental agent. Growth inhibition of 50% (GI_{50}) is calculated from $[(T_i - T_z)/(C - T_z)]\times 100 = 50$, which is the drug concentration resulting in a 50% reduction in the net protein increase.

The drug concentration resulting in total growth inhibition (TGI) is calculated from $T_i = T_z$. The LC_{50} (concentration of drug resulting in a 50% reduction in the measured protein at the end of the drug treatment is calculated from $[(T_i - T_z)/T_z]\times 100 = (-50)$.

Values are calculated for each of these three parameters if the level of activity is reached; however, if the effect is not reached or exceeded, the value for that parameter is expressed as greater or less than the maximum or minimum concentration tested [39,40].

Acknowledgments

The excellent technical support by Ilka Müller is highly appreciated. The work was supported by a grant from the Federal Ministry of Education and Research (Fö. 01KS9602) and the Interdisciplinary Center of Clinical Research Tübingen (IZKF) to V.J.

The authors thank the Antitumour Evaluation Branch and Biological Testing Branch of the NCI for performing biological evaluations.

References

[1] S.A. Aaronson, Science 254 (1991) 1146–1152.
[2] Y. Yarden, M.X. Sliwkowski, Nat. Rev. Mol. Cell Biol. 2 (2001) 127.
[3] D. Salomon, W. Gullick, Signal J. 2 (3) (2001) 4–11.
[4] M.W. Pederson, H.S. Poulson, Sci. Med. (2002) 32–43.
[5] E. Raymond, S. Faivre, J.P. Armand, Drugs 60 (1) (2000) 15–23.
[6] A. Levitzki, A. Gazit, Science 267 (1995) 1782–1788.
[7] C.L. Arteaga, J. Clin. Oncol. 19 (15) (2001) 32S–40S.
[8] F. Ciardiello, R. Caputo, R. Bianco, D. Vincenzo, G. Somatico, S. De Placido, R.A. Bianco, G. Tortora, Clin. Cancer Res. 6 (2000) 2053–2063.
[9] V. Pollack, D.M. Savage, D.A. Baker, et al., J. Pharmacol. Exp. Ther. 291 (2) (1999) 739–748.
[10] R. Albuschat, in: Doctoral Thesis, Free University of Berlin, 2003, pp. 90–93.
[11] T. Onoda, H. Iinuma, Y. Sasaki, M. Hamada, K. Isshiki, H. Naganawa, T.J. Takeuchi, J. Nat. Prod. 42 (6) (1989) 1252–1257.
[12] C.N. Hodge, J.A. Pierce, Bioorg. Med. Chem. Lett 3 (1993) 1605–1608.
[13] P. Traxler, J. Green, H. Mett, U. Sequin, P. Furet, J. Med. Chem. 42 (6) (1999) 1018–1026.
[14] G.W. Rewcastle, et al., J. Med. Chem. 38 (18) (1995) 3482–3487.
[15] J. Baselga, S.D. Averbruch, Drugs 60 (1) (2000) 33–40.
[16] V. Sherwood, A.J. Bridges, W.A. Denny, G.W. Rewcastle, J.B. Smaill, D.W. Fry, Proc. Am. Assoc. Cancer Res. 41 (2000) 3076.
[17] J.B. Smaill, et al., J. Med. Chem. 42 (10) (1999) 1803–1815.
[18] M.J. Morin, Oncogene 19 (2000) 6574–6583.
[19] P.W. Vincent, S.J. Patmore, B.E. Atkinson, A.J. Bridges, L.S. Kirkish, R.C. Dudeck, W.R. Leopold, H. Zhou, W.L. Elliott, Proc. Am. Assoc. Cancer Res. 40 (1999) 117.
[20] D.W. Fry, A.J. Bridges, A. Doherty, K. Greis, J.L. Hicks, K.E. Hook, P.R. Keller, W.R. Leopold, J. Loo, D.J. McNamara, J.M. Nelson, V. Sherwood, J.B. Smaill, S. Trumpp-Kallmeyer, E. Dobrusin, Proc. Natl. Acad. Sci. USA 95 (1998) 12022–12027.
[21] H.R. Tsou, et al., J. Med. Chem. 44 (3) (2001) 2719–2734.
[22] J.H. Billmann, J.W. McDowell, J. Org. Chem. 26 (1961) 1437–1440.
[23] E. Keller, SCHAKAL 88 A Fortran Program for the Graphical Representation of Molecular and Crystallographic Models, University of Freiburg, Germany, 1988.
[24] M.R. Grever, B.A. Schepartz, Life Sci. 57 (1995) 131–141.
[25] M.R. Boyd, K.D. Paul, Drug Dev. Res. 34 (1995) 91.
[26] W.K. Hong, A. Ullrich, Oncol Biother. 1 (1) (2000) 2–6.
[27] C.L. Sawyers, N. Engl. J. Med. 340 (1999) 1330–1340.
[28] E. Buchdunger, J. Zimmermann, H. Mett, et al., Cancer Res. 56 (1996) 100–104.
[29] N.N. Glivec, Summary of Product Characteristics, Novartis Pharma AG (2001) (imatinib).
[30] M. Carroll, S. Ohno-Jones, S. Tamura, et al., Blood 90 (1997) 4947–4952.
[31] A. Altomare, G. Cascarono, C. Giacovazzo, A. Guagliardi, M.C. Burla, G. Polidori, M. Camalli, J. Appl. Crystallogr. 27 (1994) 435.
[32] G.M. Sheldrick, SHELXL-97 A Program for Refinement of Crystal Structures Technical Report, University of Göttingen, Germany, 1997.
[33] Bruker, SMART, SAINT-Plus and SADABS, in: Data Collection and Processing Software for the SMART System, Bruker AXS, Madison, Wisconsin, USA, 2002.
[34] J.F. Geissler, P. Traxler, U. Regenass, B.J. Murray, J.L. Roesel, T. Meyer, E. McGlynn, A. Storni, N.B. Lydon, J. Biol. Chem. 265 (1990) 22255–22261.
[35] P.S. Wedegartner, G.N. Gill, J. Biol. Chem. 264 (1989) 11346–11353.
[36] P. Yaish, A. Gazit, C. Golin, A. Levitzki, Science 242 (1988) 933–935.
[37] A. Lin, MDS Pharma Services, Taiwan, R.O.C., correspondence.
[38] V. Jendrossek, B. Erdlenbruch, H. Hunold, W. Kugler, H. Eibl, M. Lakomek, Intern. J. Oncol. 14 (1999) 15–22.
[39] M.C. Alley, D.A. Scudiero, P.A. Monks, M.L. Hursey, M.J. Czerwinski, D.L. Fine, B.J. Abbott, J.G. Mayo, R.H. Shoemaker, M.R. Boyd, Cancer Res. 48 (1988) 589–601.
[40] M.R. Grever, S.A. Schepartz, B.A. Chabner, Sem. Oncol. 19 (6) (1992) 622–638.